Physical Modelling in Geotechnics – McNamara et al. (Eds)
© 2018 Taylor & Francis Group, London, ISBN 978-1-138-34422-8

A new procedure for tracking displacements of submerged sloping ground in centrifuge testing

T. Carey, N. Stone & B. Kutter
University of California Davis, Davis, California

M. Hajialilue-Bonab
University of Tabriz, Tabriz, Iran

ABSTRACT: Measuring the displacement of a sloping ground using contact sensors such as potentiometers or LVDTs is problematic because the direction of movement is not known, and the contacting forces can either reinforce the soil or affect the measurements. This is especially true if there is a possibility that sensor attachments might move in liquefied soil. Others have used image-based methods to determine displacements but capturing clear photos of an underwater soil surface has proved challenging. This paper describes the development of a new wave suppressing window and camera setup for recording displacements of a submerged slope during earthquake-induced liquefaction. The bottom of the wave suppressing window was located beneath the water surface and acted like a glass bottom boat. Five GoPro cameras recorded movement of surface markers located on the slope. The videos were converted to displacement time histories using GEOPIV and the process described herein. The displacement time histories from the cameras is consistent with relative displacements calculated by double integration of accelerometer data and with residual displacements from before-and-after hand measurements of the surface markers. Results from this analysis have shown this method for tracking displacements is extremely accurate and can be used to better understand how liquefied slopes displace during strong shaking. The camera data in turn, lend credence to a proposed method to estimate relative displacement time histories from a hybrid of accelerometer measurements, Integrated Positive Relative Velocity (IPRV) and independently measured permanent displacements.

1 INTRODUCTION

Typically, displacement transducers (LVDT), have been used to record displacements of a liquefied soil. Although, as Fiegel & Kutter (1994) observed, these sensors can reinforce soil and resist displacements during liquefaction.

GEOPIV (e.g., White et al. 2003) has been applied extensively to determine deformation patterns from images of geotechnical models. Their typical approach is to set up a camera that views a cross section of a plane-strain model through a window. Thus, friction on the window might affect the movement of soil. Kutter et al. (2017) showed several experiments where the measured displacement on the central plane was different from that on the window boundaries.

For the present project, our goal was to measure surface displacements of curved and sloping submerged ground surfaces. This raised new issues that the target surface was not entirely in the same plane nor would remain in its initial plane. Refraction of light at the air-water interface with water waves generated by shaking would distort images. Kokkali et al. (2017), successfully tracked displacements of a submerged slope and markers using a high resolution, high speed camera, noted the water waves would form at container boundaries. During especially strong shaking, the interference from waves became so severe the markers were difficult to track.

The LEAP project (Liquefaction Experiments and Analysis Projects) is an international collaboration amongst researchers to verify and validate numerical models that predict liquefaction with centrifuge experiments, and blind prediction exercises (Manzari et al. 2015). The current phase of the project, LEAP-UCD-2017 consists of 24 experiments performed at 9 different research facilities.

This paper describes a wave suppressing window developed for the LEAP-UCD-2017 experiments performed on the 1 m centrifuge at the University of Cali fornia, Davis. Five GoPro cameras were mounted on a camera and lens holder above the wave suppressing window and recorded liquefaction induced ground deformations. The recorded videos were converted to images, and using GEOPIV analysis, displacement time histories were generated. The time histories determined from the GEOPIV analysis are compared to relative displacements computed from accelerometer

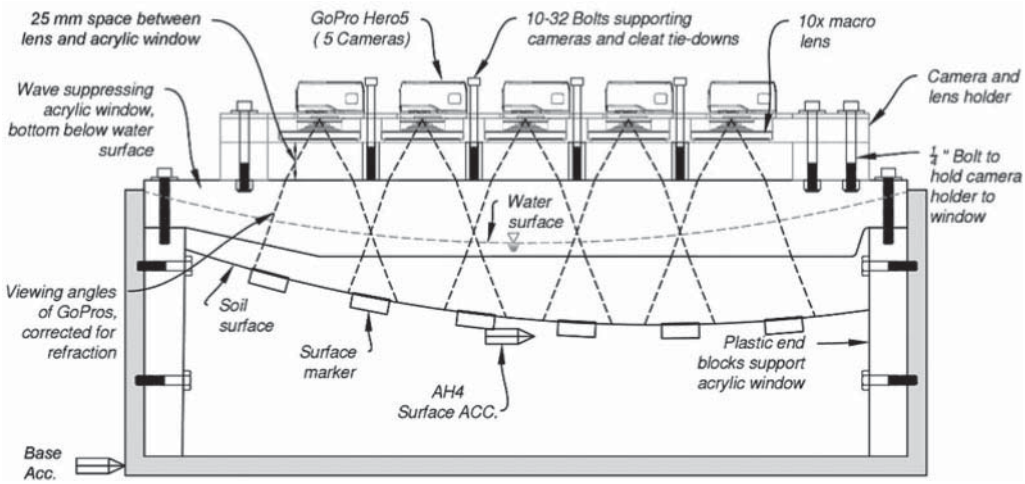

Figure 1. Elevation view of model geometry, and camera setup for UCD's LEAP-UCD-2017 centrifuge tests.

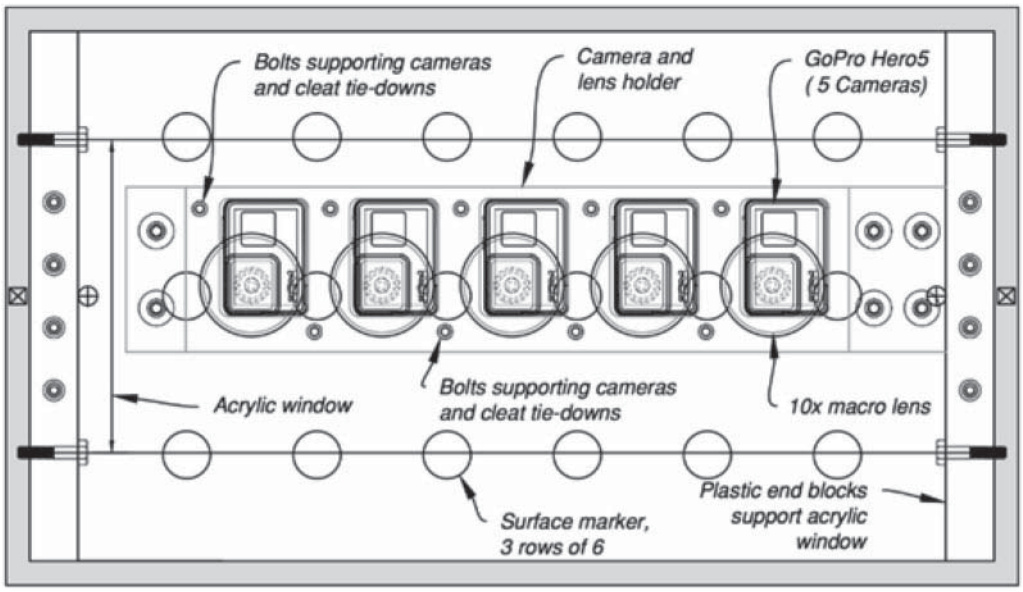

Figure 2. Plan view of model geometry, and camera setup for UCD's LEAP-UCD-2017 centrifuge tests.

data and a hybrid method that combines relative displacement, Integrated Positive Relative Velocity (IPRV) and hand measurements of markers.

2 WAVE SUPPRESSING WINDOW AND CAMERA SETUP

The wave suppressing window, and the camera setup mounted above a submerged slope are sketched in Figures 1 and 2 and photographed in Figure 3 for the LEAP-UCD-2017 test geometry. Five GoPro Hero5 cameras, each recording at 240 frames per second (fps) at 480×848p resolution, are mounted on an acrylic plate that also serves as a macro lens holder. $10\times$ macro lenses were used to record sharply focused images at distances as small as 12 cm from the camera. The lenses also permit the cameras to be positioned close to the model container allowing the cameras and lenses to be rigidly secured. By affixing the cameras close to the container, the mm/pixel resolution is improved. The proposed setup consists of three main components that were designed and manufactured from clear acrylic: 1) the wave suppressing window, 2) the lens holder, and 3) the camera holder. These components are described in detail herein.

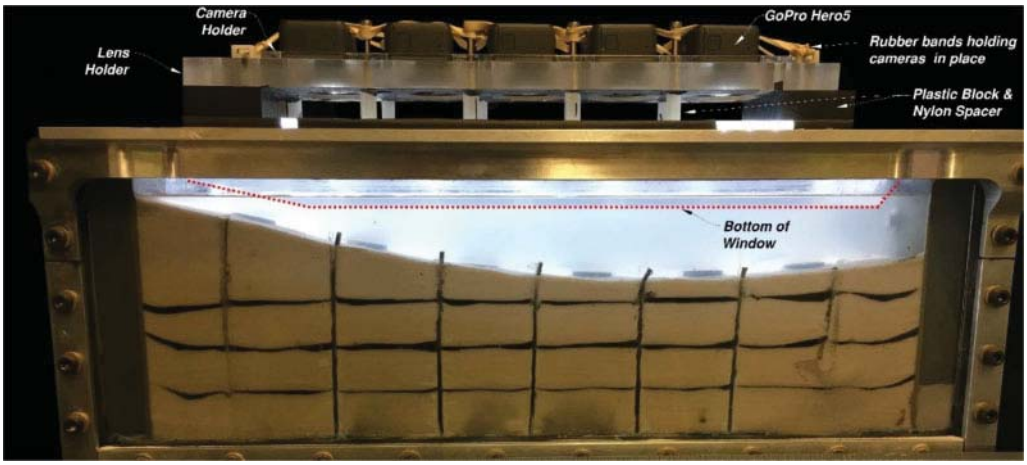

Figure 3. Photo of test geometry and camera set up on the centrifuge arm.

2.1 *Wave suppressing window*

The bottom of the wave suppressing window is below the water surface, which eliminates the air-water interface and image distortion caused by surface water waves, a similar concept to a glass bottom boat. The window is manufactured from 50 mm thick acrylic. 50 mm thickness was chosen for two reasons: first to control deflection of the window (due to the g-field and strong shaking), and to prevent an air gap from developing when the water surface curves in the radial g-field. A 12-degree taper was machined on the bottom left-hand side of the window (see Figure 1) to avoid interference with the sloping ground surface in this specific experiment. The tapered surface was polished for optical clarity. To alleviate dynamic water pressures, caused by sloshing of water during shaking, the wave suppressing window does not cover the entire model. The window and longitudinal walls of the container are separated by a 57 mm gap. On each end of the container are 25 mm thick plastic end blocks that support the window.

2.2 *Camera setup*

Figure 4 shows a detailed view of a single GoPro camera and lens. The lens holder was machined to provide a snug fit for the macro lens and prevent movement of the lens during shaking.

The GoPro cameras rest atop the lens holder plate and are retained laterally by a 3 mm thick acrylic camera holder plate. Gasket tape was applied to the holder to prevent the cameras from moving in the holder. Rubber bands (Figure 3) are laced over the cameras to hold them snuggly in the camera holder against the top of the lens holder plate.

The camera and lens holder are located 25 mm above the window, a distance determined to provide the desired field of view, accounting for refraction of the lens, and at the air/plastic/water interfaces. The experiment required 18 surface makers to be placed

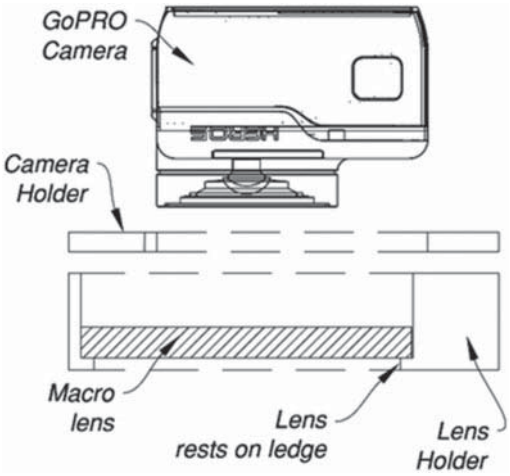

Figure 4. Detailed view of camera and lens holder.

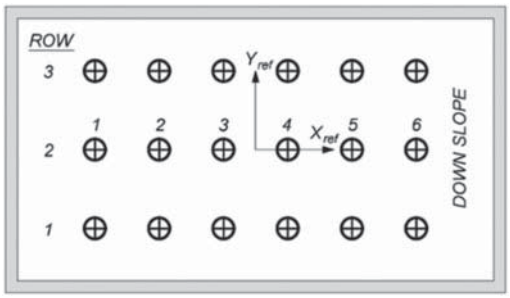

Figure 5. Surface marker locations for the LEAP-UCD-2017.

in 3 rows of 6 markers. A schematic of the locations of the 25 mm diameter markers is shown in Figure 5. The setup was designed to allow markers 2, 3, 4, and 5 in all three rows to be viewed by two cameras located

up and down slope of the marker. For example, the middle camera will record the movement of markers 3 and 4, and the camera to the right will record markers 4 and 5. So, these two cameras both provide independent images of marker 4. Markers 1 and 6 are only recorded by the far left and far right cameras, respectively.

GoPro cameras were selected for their ruggedness, size, and low cost compared with other high-speed cameras. The GoPro cameras record at 240 fps, roughly corresponding to 5.5 frames per cycle of shaking of the model earthquake, which, for this experiment was a tapered sine wave with predominant frequency of 43.75 Hz, model scale. 5.5 frames per cycle of shaking was considered sufficient to quantify the cyclic component of dynamic deformation.

An instrumented calibration test was performed to confirm that the camera/lens/window mounting was rigid enough. Accelerometers were placed on the container, wave suppressing window, and camera holder measuring both vertical and horizontal components. The movements of the cameras and waver suppressing window, relative to the model container, were determined to be negligible.

3 PIV ANALYSIS

GEOPIV-RG is an image-based tool for measuring displacements and has been extensively used for geotechnical and centrifuge applications (Stanier et al. 2015). The current version of GEOPIV-RG is more precise by a factor of ten compared with its predecessors (Stanier et al. 2015), providing subpixel resolution.

Figure 6 is a typical image from one of the cameras. The gray areas around the edges of the photos are exclusion zones for the present analysis. The region that is not grayed out is the region of interest, which is divided into 150 × 150 pixel zones, spaced at 100 pixels. Overlapping of the zones ensures full coverage of the surface. A seed point, indicated in Figure 6, serves a fixed reference location for the zones. The seed point was selected as an LED reflection off the water-window interface. The LEDs and camera were firmly attached to the top of the suppressing window, so the LED reflection point is not expected to move relative to the camera. Analysis was performed using the Eulerian analysis mode.

Using Eulerian analysis method, GEOPIV provides the displacement of each zone in units of pixels. To scale pixels to mm, a conversion factor for each marker in each camera was found by determining the length, to the nearest whole pixel, of the surface marker from the image similar to Figure 6 prior to shaking. For example, if the 25 mm diameter surface marker in Figure 6 is 100 pixels across, the scale factor would be 0.25 pixel/mm. The typical scale factors ranged from about 0.2 to 0.25 pixel/mm for all the cameras depending on the distance between the markers and the camera. The GEOPIV analysis was performed over the entire region shown in Figure 6, but only patches corresponding to the locations of surface markers were processed. This allows the use of discrete conversion factors rather than a continuous function across the image, which have been used by others (White et al. 2003) for conversion. This method of scaling introduces small errors from pixel counting.

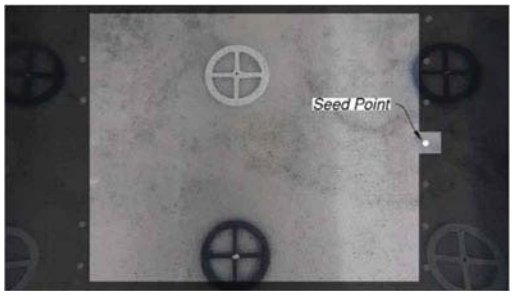

Figure 6. A typical view of a camera looking through the window. The gray area is the exclusion zone, the potions of the frame the GEOPIV software does not track displacements.

4 RESULTS

As part of the LEAP-UCD-2017 exercise, the research team at UC Davis performed 3 centrifuge experiments, with multiple shaking events per experiment. The data presented herein is from one of those shaking events. The model consisted of a uniform Ottawa F-65 sand profile inclined at 5 degree slope. The depth of the model at the midpoint of the container is 4 m in prototype scale. The scale factor ($L^* = L_{model}/L_{prototype}$) for this experiment is 1/43.75.

Figure 7 compares the relative displacement obtained from processing accelerometer data to that from the GEOPIV analyses. The relative displacement from the accelerometers is the difference of the double integrated acceleration time histories of the base and AH4 accelerometers (Figure 1) and is reliable for use as validation of the GEOPIV analysis. Following integration, calculated displacement drift was removed by filtering the displacement time histories with a high pass filter with a corner frequency of 8.75 Hz, a process known as "baseline correction". Baseline correction of displacements obtained from accelerometers is necessary because accelerometers are insensitive to long duration, slow displacements. The displacement data from the GEOPIV analysis was also filtered using a high pass filter with a corner frequency of 8.75 Hz. The predominant frequency of the model earthquake was 43.75 Hz, so the 8.75 Hz filtering of the GEOPIV analysis and relative displacement from the accelerometers would not affect the cyclic displacements and the analysis methods could be compared in Figure 7.

Good agreement can be observed for the two methods for determining relative displacements. Surface markers 3 and 4 are the best comparison of the two methods since the surface accelerometer AH4 is located between the two markers. Markers 1 and 5 are

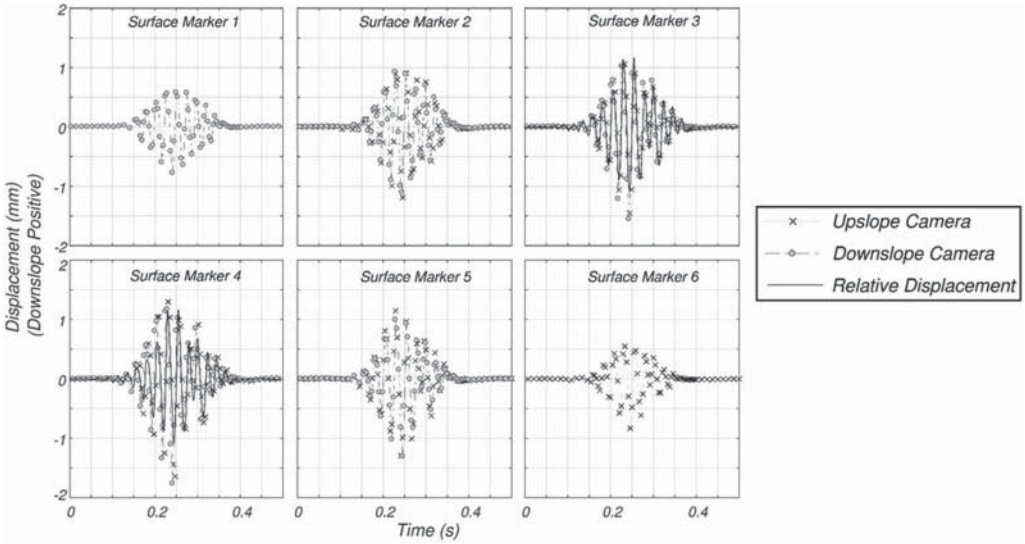

Figure 7. Relative displacement calculated from accelerometers and GEOPIV for markers 3 and 4.

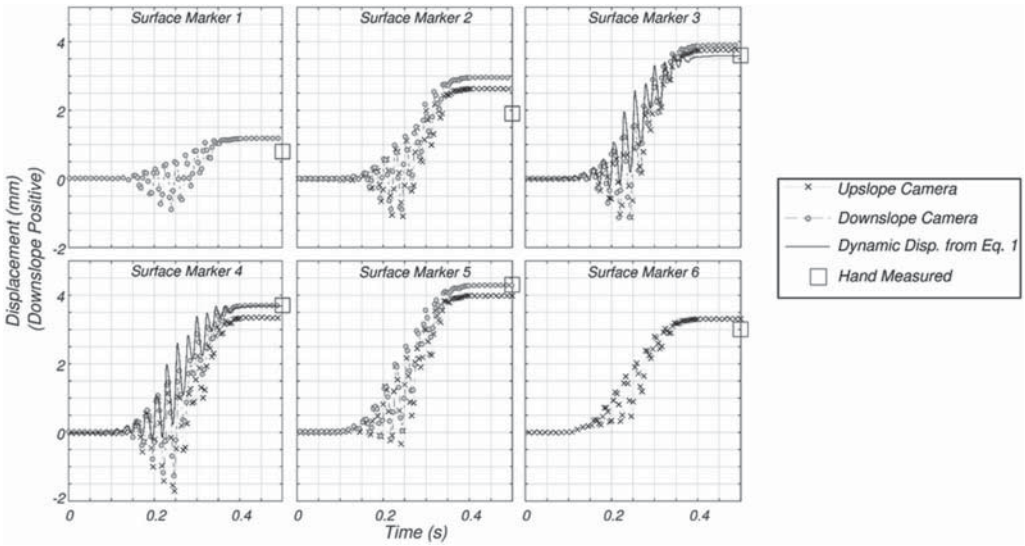

Figure 8. GEOPIV displacement time histories and displacement from IPRV and accelerometer data.

expected to move less than Markers 3 and 4, because they are closer and more restricted by the end wall boundaries of the rigid model container.

Shown in Figure 8 are the unfiltered GEOPIV displacement time series with the residual displacements. Independent hand measurements of marker displacements using rulers and calipers after stopping the centrifuge are indicated by the large square on the right side of each figure. In most cases, the residual displacement from the GEOPIV analysis agrees with the hand measurements of surface markers and are within 0.5 mm, consistent with the accuracy of the hand measurements. Also, in Figure 8, the curve labeled "From IPRV & Accelerometers" uses a process described by Kutter et al. (2017). The IPRV (Integrated Positive Relative Velocity) is defined as,

$$IPRV = \int_0^\infty \chi[v_{rel}(t)]dt \quad (1)$$

$$where\ \chi = \begin{cases} 0 & if\ \ v_{rel}(t) < 0 \\ 1 & if\ \ v_{rel}(t) > 0 \end{cases}$$

where v_{rel} is the relative velocity. This function produces a reasonable shape of the accumulation ramp of the permanent displacements. The IPRV ramp function is then scaled to make it agree with the hand measurements of the surface marker displacement. The "From IPRV & Accelerometers" curves were obtained

by adding the cyclic displacement from the accelerometers (data shown in Figure 7) to the scaled IPRV ramp.

Overall, good agreement can be observed with GEOPIV and curves determined using accelerometer data with the IPRV ramp. It appears that the IPRV ramp predicts that displacements accumulate earlier in the time series then the PIV analysis. In other words, the first few significant cycles of displacement from the GEOPIV analysis show negligible accumulation of permanent displacement, but the IPRV ramp does accumulate residual displacements in every cycle of relative displacement. The IPRV function does not account for the effect of liquefaction on the shape of the residual displacement ramp, but nevertheless, the IPRV function does allow a reasonable visualisation of the displacement time series data that could be useful in the absence of image analysis data.

5 CONCLUSION

A new device and procedure was developed to track dynamic and residual displacements of a submerged sloping liquefied ground using the software GEOPIV. The device consisted of a wave suppressing window, functioning like a glass bottom boat, that allowed clear images to be obtained by looking vertically down at a submerged sloping surface. Attached to the window was a camera holder, with five GoPro Hero5 cameras recording at 240 fps, and a lens holder with 10x macro lenses, allowing the cameras to be located a short distance from the soil surface. Video recorded during shaking was converted to pixel displacements using GEOPIV. Pixel displacements of surface markers were converted to units of mm using a variable scale factor determined by the length of the surface markers (25 mm) and the number of pixels occupied by the surface markers. This accounted for distortion of the image and variable distance of the markers to the camera.

The cyclic components of displacements from the GEOPIV analysis were filtered to remove permanent deformations and compared well with cyclic displacements calculated from the accelerometer data. The permanent displacements from unfiltered GEOPIV displacements also compared well (usually within about 0.5 mm) to the hand measurements of displacements of surface markers. A method to generate displacement time histories from acceleration data, using the Integrated Positive Relative Velocity (IPRV) to determine the shape of the ramp defining the accumulation or permanent displacement provided a reasonable approximation to the data from GEOPIV.

It has been difficult in centrifuge model testing to measure permanent displacements of submerged liquefying slopes. The use of several cameras viewing through a wave suppressing window along with techniques described herein allows high resolution dynamic displacement data to be obtained at a multitude of points across a submerged sloping ground surface.

ACKNOWLEDGMENTS

Funding for this work was provided by the National Science Foundation under CMMI grant 1635307. The authors would also like to thank Dr. Dan Wilson and the CGM stuff for their review, advice and assistance with this work.

REFERENCES

Fiegel, G.L. and Kutter, B.L., 1994. Liquefaction mechanism for layered soils. *Journal of geotechnical engineering*, 120(4), pp. 737–755.

Kokkali, P., Abdoun, T., Zeghal, M., 2017. Physical modeling of soil liquefaction: Overview of LEAP production test 1 at Rensselaer Polytechnic Institute. *Soil Dynamics and Earthquake Engineering*.

Kutter, B.L., Carey, T.J., Hashimoto, T., Zeghal, M., Abdoun, Madabhushi, S.P.G., Haigh, S.K., Burali d'Arezzo, F., Madabhushi, S.S.C., Hung, W.-Y., Lee, C.-J., Cheng, H.-C., Iai, S., Tobita, T., Ashino, T., Ren, J., Zhou, Y.-G., Chen, Y., Sun, Z.-B., & Manzari, M.T. 2016. LEAP-GWU-2015 Experiment Specifications, Results and Comparisons. *Soil Dynamics and Earthquake Engineering*.

Manzari, M., B. Kutter, M. Zeghal, S. Iai, T. Tobita, S. Madabhushi, S.K. Haigh, L. Mejia, D. Gutierrez, R. Armstrong, M. Sharp, Y. Chen, & Y. Zhou. 2014. Leap projects: concept and challenges. In *Geotechnics for catastrophic flooding events*, pp. 109–116. CRC Press.

Stanier, S.A., Blaber, J., Take, W.A. and White, D.J., 2015. Improved image-based deformation measurement for geotechnical applications. *Canadian Geotechnical Journal*, 53(5), pp.727–739.

White, D.J., Take, W.A. and Bolton, M.D., 2003. Soil deformation measurement using particle image velocimetry (PIV) and photogrammetry. *Geotechnique*, 53(7), pp. 619–631